03,07,10

Ab initio calculation of the structure and frequency dependences of dielectric properties of new semiconductors $TlIn_{1-x}Tm_xS_2$ ($x = 0.001$ and 0.005)

© S.N. Mustafaeva[1], S.M. Asadov[2,3] S.S. Huseynova[1,4]

[1] Institute of Physics Ministry of Science and Education Republic of Azerbaijan,
Baku, Azerbaijan
[2] Nagiyev Institute of Catalysis and Inorganic Chemistry, Ministry of Science and Education Republic of Azerbaijan,
Baku, Azerbaijan
[3] Scientific Research Institute „Geotechnological Problems of Oil, Gas and Chemistry"
of Azerbaijan State Oil and Industry University,
Baku, Azerbaijan
[4] Khazar University,
Baku, Azerbaijan

E-mail: solmust@gmail.com

Received February 3, 2024
Revised February 3, 2024
Accepted February 4, 2024

The monoclinic structure $TlIn_{1-x}Tm_xS_2$ was studied based on the density functional theory (DFT). The cases of substitution of indium atoms with thulium are considered. The lattice cell parameters were determined in optimized supercells $TlInS_2$ taking into account the approximation of the local density. Lattice constants for a layered crystal $TlIn_{1-x}Tm_xS_2$ were theoretically determined based on calculations of a monoclinic structure with a space group $C/2c$ (coordination number $Z = 16$, № 15) and compared with experimental results. New semiconductor polycrystals of $TlIn_{1-x}Tm_xS_2$ ($x = 0$, 0.001 and 0.005) compositions were synthesized in quartz ampoules and corresponding single crystals were grown from them by directional solidification method. Analysis of X-ray diffraction patterns shows that all compositions $TlIn_{1-x}Tm_xS_2$ have stable monoclinic crystal system with space group $C/2c$. The calculated parameters of the lattice cell of $TlIn_{1-x}Tm_xS_2$ samples confirm this. Dielectric properties in alternating electric fields with a frequency of $f = 5 \cdot 10^4 - 3.5 \cdot 10^7$ Hz at room temperature were studied in single crystals. The relaxation character of the dielectric constant, the nature of dielectric losses, and the hopping mechanism of charge transfer in $TlIn_{1-x}Tm_xS_2$ samples were determined. The parameters of localized states in crystals of $TlIn_{1-x}Tm_xS_2$ samples were calculated using the Mott model. It was shown that, the AC conductivity, the density of localized states near the Fermi level, the average distance and time of charge carrier hops in $TlIn_{1-x}Tm_xS_2$ increase compared with the undoped $TlInS_2$.

Keywords: monoclinic structure, DFT LDA, single crystal $TlInS_2$, doping impact, thulium impurity, lattice cell parameters, permittivity, hopping conductance, frequency dispersion, dielectric losses.

DOI: 10.61011/PSS.2024.04.58195.8

1. Introduction

Doped phases based on layered crystals of compounds of the $TlB^{III}C_2^{VI}$ group, having high photosensitivity, are promising ferroelectric and semiconductor materials. They can be used as active materials for infrared and visible range, X-ray and gamma-ray sensors, memory elements, etc. [1–19]. The properties of these compounds significantly depend on the parameters of the doping components, the chemical composition and structure of the matrix (crystal size, morphology, fraction of the crystalline phase), as well as processing conditions. In particular, materials based on the triple compound $TlInS_2$ that have a layered structure are characterized by anisotropy of physical properties and have a strong potential for application as active elements of semiconductor devices [1–19]. The crystal structure of the $TlInS_2$ compound is characterized by the formation of several polymorphic modifications [1,2]. At least five stable polymorphous modifications of the $TlInS_2$ compound have been reported: monoclinic [3–5], rhombic [4], tetragonal [6], hexagonal [7] and triclinic [8].

The structure features affect the physical properties of $TlInS_2$ [9–19]. This is confirmed, in particular, by the results of the study of the temperature dependence of the degree of anisotropy of the direct current conductivity of $TlInS_2$ single crystals [9]. The results of low-temperature (100–300 K) X-ray studies of the $TlInS_2$ single crystal indicate that the parameters of the crystal lattice cell gradually increase with the increase of the temperature [10]. Anomalies in the form of kinks and breaks are observed on the temperature dependence curves of the lattice parameters at temperatures corresponding to phase transitions in $TlInS_2$. The coefficient of linear thermal expansion α along the crystallographic direction [001] of the TlInS crystal$_2$ is determined. The

value of the coefficient α slightly changes with an increase of the temperature. The dielectric properties and alternating current conductivity (AC conductivity) of the single crystal of the $TlInS_2$ compound also markedly change under the impact of doping with trivalent rare earth ions of *Re* [11]. However, the patterns of influence of the composition on the properties of doped layered crystals based on $TlInS_2$ have been little studied.

There are few papers devoted to the study of crystallization processes and properties of doped $TlInS_2$ containing *Re*. The addition of an impurity, for example, erbium (Er) significantly improves dielectric properties of $TlInS_2$ [11] crystals. A significant alteration of the properties of crystals based on $TlInS_2$, in particular, can be associated with the modification of the band structure owing to the partial cationic substitution when Er^{3+} is introduced into the $TlInS_2$ crystal lattice. TlInS crystals doped with trivalent rare earth ions of Re^{3+} have been insufficiently studied.

The formation of new electronic materials with a given set of physical and chemical characteristics is associated with the study of multicomponent alloys including doping elements. At the same time, interatomic distances and the nature of exchange interactions can be varied in substitutional alloys, resulting, for example, in structural ordering, as well as to phase transformations in $TlInS_2$ [12–18]. These phenomena depend significantly on the size of impurity and type of impurity substitution, for example, *Re*. Therefore, a comprehensive study of the structure and physical properties of $TlInS_2$ containing *Re* is a relevant objective.

It is also unclear which physical and chemical mechanisms are responsible for the formation of sensitive parameters (dielectric coefficients, photoluminescence, etc.) in case of cationic substitution of Re^{3+} in the $TlInS_2$ crystal lattice.

The purpose of this paper is to study the impact of thulium dopant ($x = 0.001$ and 0.005) on the structure and dielectric properties of grown single crystals of $TlInS_2$ of monoclinic modification using calculations based on the density functional theory (DFT). The second objective is the study of the mechanism of charge transfer in samples of $TlIn_{1-x}Tm_xS_2$ ($x = 0.001$ and 0.005) in alternating electric fields of the radio frequency range at room temperature.

2. Methodological part

2.1. DFT-calculation of lattice constants

The ATK software package based on density functional theory was used. Electronic configurations of $TlIn_{1-x}Tm_xS_2$ components were considered in DFT calculations: Tl — $[Xe]\,4f^{14}5d^{10}6s^26p^1$, In — $[Kr]\ 4d^{10}5s^25p^1$, S — $[Ne]\,3s^23p^4$ and impurity Tm — $[Xe]\,4f^{13}6s^2$. DFT calculations of the lattice constants of $C/2c$ monoclinic structure with the coordination number $Z = 16$ of supercells based on $TlInS_2$ were performed. Crystal supercell structure was optimized by changing the position of the atoms of the components of $TlIn_{1-x}Tm_xS_2$, the shape and volume of the lattice cell. The cutoff energy of the plane wave in the calculations of the self-consistent field was 300 eV. We used *k*-point generation scheme based on the Monkhorst-Pack method with a flat grid with a dimension of $4 \times 4 \times 2$ points for the Brillouin zone of a monoclinic structure (Figure 1). This ensures the convergence of the method with the lattice cell total energy of $\geq 5 \cdot 10^{-6}$ eV/atom. The convergence threshold for the interatomic forces was 10^{-4} eV/Å.

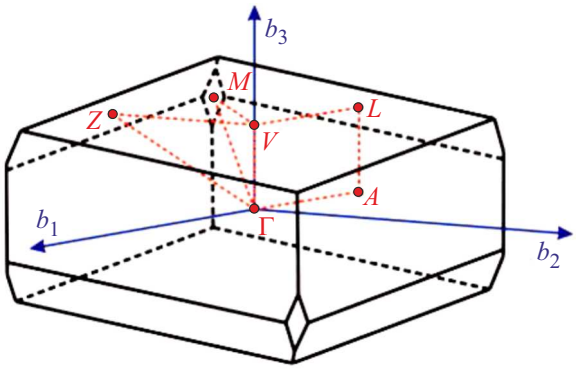

Figure 1. The scheme of the first Brillouin zone of the crystal lattice of the basocentric monoclinic symmetry for $TlInS_2$.

It was assumed in the DFT calculations that the $TlInS_2$ compound crystallizes in a centered monoclinic lattice with a space symmetry group $C/2c$, $Z = 16$ and has four formula units per primitive cell containing 32 atoms. Figure 2 shows a primitive lattice cell based on $TlInS_2$ crystals, calculated using the DFT method.

2.2. Preparation of samples and experiment details

The following chemical elements were used as parent elements: Tl (Tl-00), In (In-000), S (high purity 16-5), Tm (99.99%). Polycrystalline samples of $TlIn_{1-x}Tm_xS_2$ ($x = 0$, 0.001 and 0.005) compositions were synthesized from elements taken in stoichiometric quantities according to the procedure described in [11,19]. The components were directly fused in quartz ampoules vacuumed up to 10^{-3},Pa in an electric furnace. Ampoules with samples were initially heated at a rate of 20−30 K/h to a temperature of 720 K and were held at this temperature for 24 h. Then the temperature of the ampoule was increased to 1050 K (melting point of $TlInS_2$ $T_m = 1040$ K) and it was maintained for 5 h. Further, ampoules with samples were cooled to room temperature at a rate of 10−20 K/h. Homogenizing annealing of synthesized polycrystalline samples of $TlIn_{1-x}Tm_xS_2$ ($x = 0$, 0.001 and 0.005) was performed in vacuum 10^{-3} Pa at 670 K during 120 h. The ampoules with samples were quenched in cold water after annealing. Differential thermal analysis (DTA) with a thermal analyzer STA 449 F3 Jupiter and X-ray phase analysis (XRA) were used to control the completeness of the synthesis of samples of $TlIn_{1-x}Tm_xS_2$, their homogeneity and individ-

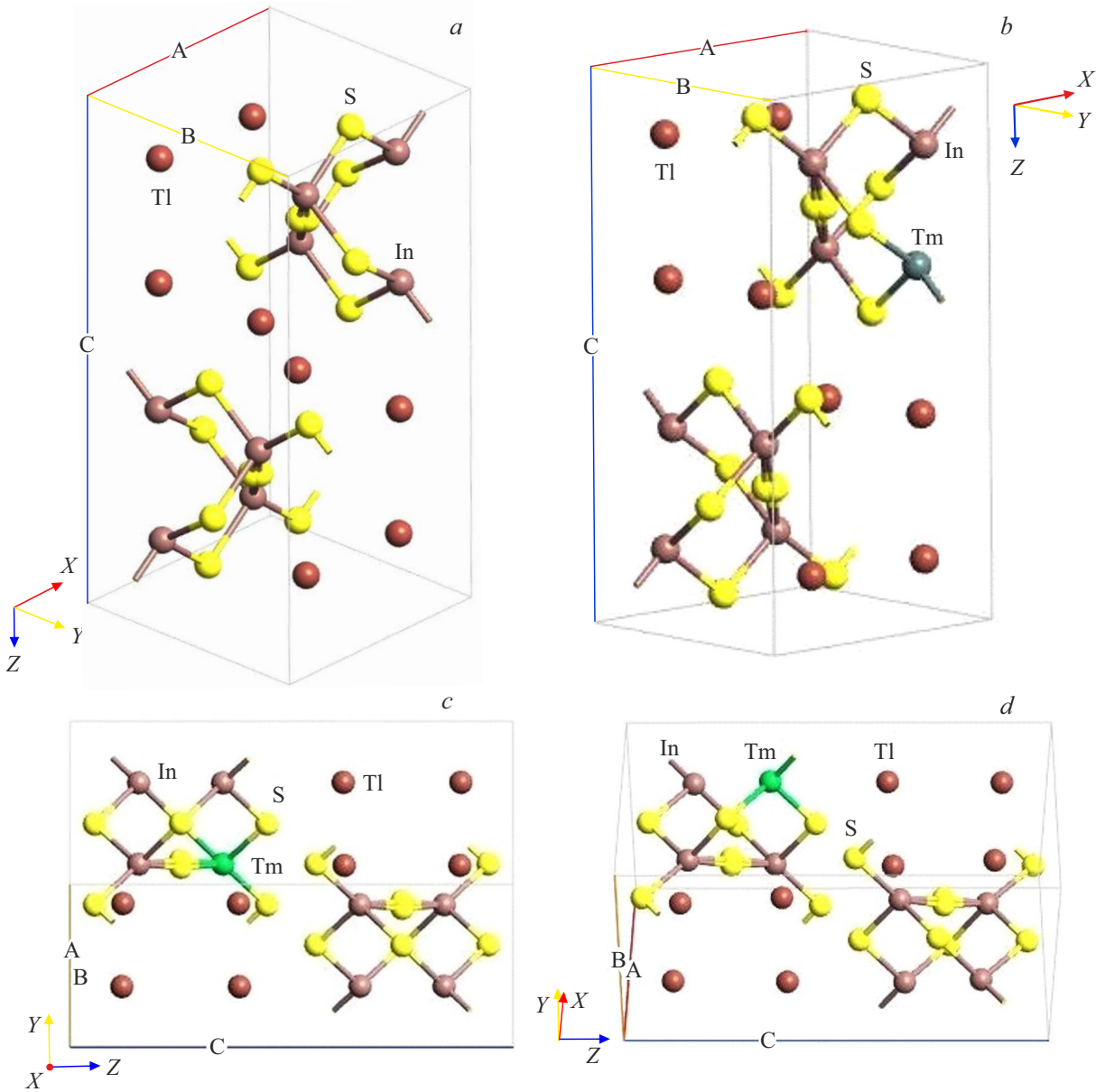

Figure 2. Optimized structures of supercells based on $TlInS_2$ crystals, obtained by us from *ab initio* calculations using the DFT method in the LDA: *a* — a primitive cell of a $TlInS_2$ crystal with monoclinic symmetry (space group $C/2c$, $Z = 16$); *b, c, d* — a primitive cell of a $TlInS_2$ crystal, including Tm, with monoclinic crystal system.

uality. X-ray images of powdered samples were acquired using D8-ADVANCE type diffractometer (CuK_α-radiation, $\lambda = 1.5418$ Å) in the $0.5° < 2\theta < 80°$ mode at 40 kV and 40 mA. Powder samples of $TlIn_{1-x}Tm_xS_2$ were prepared from synthesized crystals of $TlIn_{1-x}Tm_xS_2$ in an agate mortar. X-ray images of synthesized samples were analyzed using the IJCD PDF-4 database and experimental values of $TlInS_2$ lattice constants at room temperature.

Single crystals of samples of $TlIn_{1-x}Tm_xS_2$ ($x = 0$, 0.001 and 0.005) compositions were grown using the vertical Bridgman-Stockbarger method [11,19]. Pre-synthesized polycrystals of $TlIn_{1-x}Tm_xS_2$ in quartz growth ampoules with a length of 30 mm and a diameter of 9 mm with a bottom in the form of a cone and vacuumed up to 10^{-3} Pa were subjected to directional solidification. A polycrystalline sample of a given $TlIn_{1-x}Tm_xS_2$ composition weighing 10 g was loaded into an ampoule, which was vacuumed and sealed. Then the ampoule with the sample was put in a tubular vertical two-zone electric furnace of a crystal growing plant. The temperature of each of the two zones of the furnace (hot zone — ≤ 1050 K, growth zone — ≤ 1040 K) was adjusted separately from each other. The accuracy of maintaining the temperature inside the two-zone furnace was ± 0.5 K. The temperature gradient at the crystallization front during cultivation was 2–3 K/min. The maximum temperature of the hot zone of the furnace was 1050 K

(10 K higher than T_m of $TlInS_2$ compound). The growth rate (crystallization front velocity) of the single crystal was 0.1−0.2 mm/h. A polycrystalline sample of $TlIn_{1-x}Tm_zS_2$ ($x = 0$, 0.001 and 0.005) composition in an ampoule placed in the hot zone of the furnace was melted and aged for 1−2 h. Then the ampoule with the melt was transferred from the hot zone into the growth zone at a rate of 10 mm/h and single crystals of $TlIn_{1-x}Tm_xS_2$ were grown. Then both zones of the furnace were simultaneously cooled at the rate of 20−30 K/h to 700 K and single crystals were annealed for 100 h at this temperature. The annealed single crystals were cooled to room temperature in the off-furnace mode. Thus, homogeneous dark orange single crystals of $TlIn_{1-x}Tm_xS_2$ ($x = 0$, 0.001 and 0.005) were obtained.

The dielectric properties and conductivity were measured on single crystal samples of $TlIn_{1-x}Tm_xS_2$ ($x = 0$, 0.001 and 0.005). Samples for electrophysical studies were made in the form of flat capacitors. Microscopic analysis (Zeiss KL1500 microscope) showed that the samples were of high quality and did not contain any microinclusions. The alignment of the samples relative to the crystallographic axes was not carried out, since the crystals of $TlIn_{1-x}Tm_xS_2$ belong to the monoclinic crystal system and are characterized by a layered structure. They easily chipped along the basic plane of the crystal.

Leitsilber silver paste was applied as electrodes on the surface of the samples of $TlIn_{1-x}Tm_xS_2$. The thickness of the samples was 0.02−0.09 cm. The dielectric coefficients of the samples were measured using the resonance method [11,19]. The frequency range of the alternating electric field was $5 \cdot 10^4 - 3.5 \cdot 10^7$ Hz. The dielectric properties were measured in the direction perpendicular to the layers of crystals of $TlIn_{1-x}Tm_xS_2$. All the dielectric measurements were carried out at 300 K. The reproducibility of the resonance position was ±0.2,pF in terms of capacitance, and $(Q = 1/\operatorname{tg}\delta) \pm 1.0-1.5$ of scale divisions in terms of quality factor. The largest deviations from the average values were 3−4% for the dielectric constant ε' and 7% for the tangent of dielectric loss angle $\operatorname{tg}\delta$.

3. Results and discussion

3.1. Structure of doped samples

The wave function for a system consisting of N electrons is calculated taking into account the spatial and spin coordinates of the electrons. In particular, a function depending on three spatial variables of the electron density $\rho(\mathbf{r})$ is used in DFT. In this case, the total energy functional is written in a known manner [11]:

$$E[\rho(\mathbf{r})] \equiv \int V_0(\mathbf{r})\rho(\mathbf{r})d\mathbf{r} + T_S[\rho(\mathbf{r})] + \frac{1}{2}\int \frac{\rho(\mathbf{r})\rho(\mathbf{r}')}{|\mathbf{r}-\mathbf{r}'|}d\mathbf{r}d\mathbf{r}' + E_{XC}[\rho(\mathbf{r})]$$

Table 1. DFT-optimized parameters of the crystal structure of $TlIn_{0.999}Tm_{0.001}S_2$ with monoclinic crystal system (space group $C2/c$, $Z = 16$, № 15) in comparison with experimental data of the crystal structure of $TlInS_2$

Parameters lattices, Å	Calculation using the DFT method in the LDA, $TlIn_{0.999}Tm_{0.001}S_2$	Experiment, $TlInS_2$		
		This paper	[4]	[12]
a	10.901	10.9017	10.95	10.90
b	10.945	10.9412	10.95	10.94
c	15.181	15.1809	15.14	15.18

where $V_0(\mathbf{r})\rho(\mathbf{r})d\mathbf{r}$ — potential of Coulomb attraction of electrons to nuclei, $T_S[\rho(\mathbf{r})]$ — kinetic energy, $\int \frac{\rho(\mathbf{r})\rho(\mathbf{r}')}{|\mathbf{r}-\mathbf{r}'|}d\mathbf{r}d\mathbf{r}$ — Coulomb interelectronic interactions, $E_{XC}[\rho(\mathbf{r})]$ — the other contributions to interelectronic interactions (exchange-correlation potential). The results of DFT calculations, in particular for semiconductors, strongly depend on the type of exchange-correlation potential E_{XC}, which characterizes multiparticle interactions.

We used the exchange-correlation functional E_{XC} in DFT calculations in the local density approximation (LDA). Calculations using the E_{XC} functional in the generalized gradient approximation (GGA) with PBE parameterization slightly overestimate the values of the $TlInS_2$ lattice constant. This is due to the fact that both the local value of the electron density and its gradient are taken into account in the GGA approximation when calculating the potential E_{XC} [19].

Optimized structures of supercells based on $TlInS_2$ crystals, obtained by us from calculations using the DFT method in the LDA, indicate that they have monoclinic crystal system with lattice cell parameters $a = 10.901$, $b = 10.945$, $c = 15.181$ Å (space group $C/2c$, $Z = 16$, № 15), consistent with the XPA data.

Substitution of an indium atom with a thulium atom in the structure of pure $TlInS_2$ (Figure 2, *a, b, c, d*) does not significantly change the parameters of the crystal lattice (Table 1).

The analysis of powder samples of $TlIn_{1-x}Tm_xS_2$ ($x = 0.001$ and 0.005) using XPA method showed that they, like $TlInS_2$, have a monoclinic structure with space symmetry group $C/2c$. The absence of impurity reflexes on the X-ray images indicates that the samples do not contain other phases. The available diffraction reflexes on X-ray images of samples $TlIn_{1-x}Tm_xS_2$ ($x = 0$, 0.001 and 0.005) correspond to the monoclinic phase of $TlInS_2$. The samples do not contain reflexes of other phases up to the composition of $x = 0.005$.

The parameters of the lattice cell of the obtained doped single crystals of $TlIn_{1-x}Tm_xS_2$ ($x = 0$, 0.001 and 0.005) within the limits of experimental accuracy coincide with the parameters of the $TlInS_2$ lattice cell. Known data on the structural characteristics of the $TlInS_2$ compound are provided in Table 1 for comparison. It is apparent that the

lattice constants of the monoclinic phase based on $TlInS_2$ are consistent with the literature data. Therefore, it was found that the parameters of the lattice cell of the doped semiconductor $TlIn_{1-x}Tm_xS_2$ are practically the same in case of the change of the composition from $x = 0.001$ to $x = 0.005$.

3.2. Dielectric properties

Figures 3–7 shows the results of measurements of the frequency dependences of the real ε' and imaginary ε'' parts of the complex dielectric permittivity, the tangent of the dielectric loss angle $\mathrm{tg}\,\delta$ and the alternating current conductivity of single crystals $TlIn_{1-x}Tm_xS_2$ ($x = 0$, 0.001 and 0.005), performed at room temperature.

Figure 3 shows that the dependence $\varepsilon'(f)$ for $TlIn_{1-x}Tm_xS_2$ was characterized by a more noticeable variance compared to $TlInS_2$ in the entire studied frequency range. An increase of the concentration of thulium dopant in crystals resulted in a noticeable increase of ε' (more than three times) as shown in Figure 4. Frequency dependences of the imaginary part of the complex dielectric permittivity ε'' of $TlIn_{1-x}Tm_xS_2$ samples indicate relaxation dispersion (Figure 5).

Figure 6 shows for comparison the frequency dependences of the tangent of the dielectric loss angle $\mathrm{tg}\,\delta$ in „pure“ crystal of $TlInS_2$ (curve *1*) and thulium-doped crystal of $TlIn_{1-x}Tm_xS_2$ with thulium concentration of $x = 0.005$ (curve *2*). The hyperbolic decline of $\mathrm{tg}\,\delta$ indicates losses of reach-through conductivity in the studied samples of $TlIn_{1-x}Tm_xS_2$. The introduction of thulium into the $TlInS_2$ lattice resulted in a significant increase of $\mathrm{tg}\,\delta$.

Figure 7 shows the constructed frequency dependence of alternating current conductivity σ_{ac} (AC conductivity) of

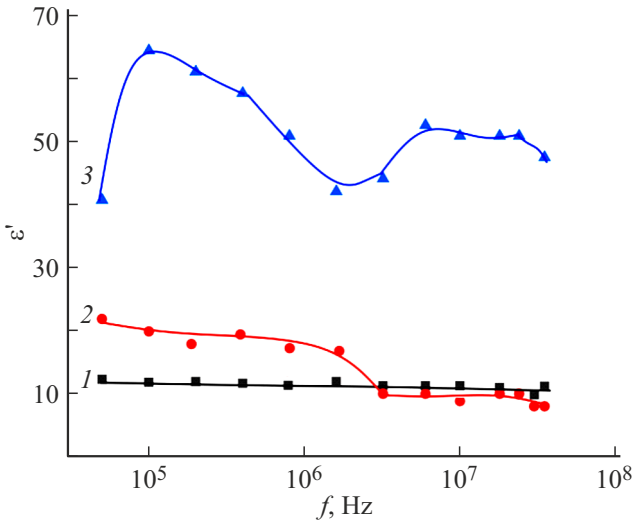

Figure 3. The frequency dependences of the real component of the complex dielectric permittivity of crystals of $TlIn_{1-x}Tm_xS_2$ of various compositions: $x = 0$ (*1*), 0.001 (*2*) and 0.005 (*3*); $T = 298$ K.

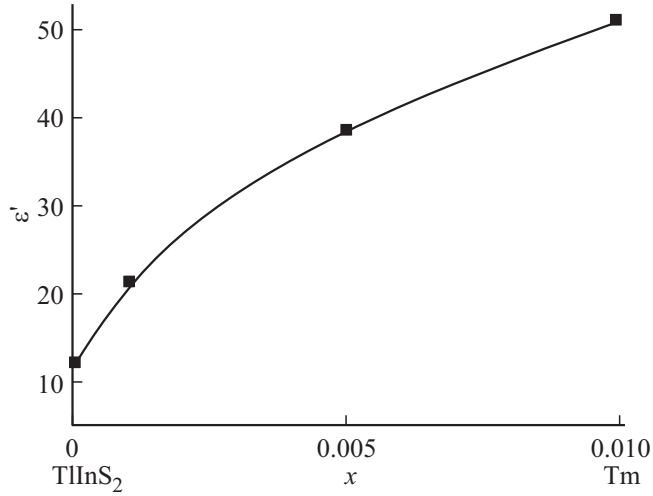

Figure 4. The dependence of the real component of the complex dielectric permittivity of crystals of $TlIn_{1-x}Tm_xS_2$ on their composition at $f = 5 \cdot 10^4$ Hz; $T = 298$ K.

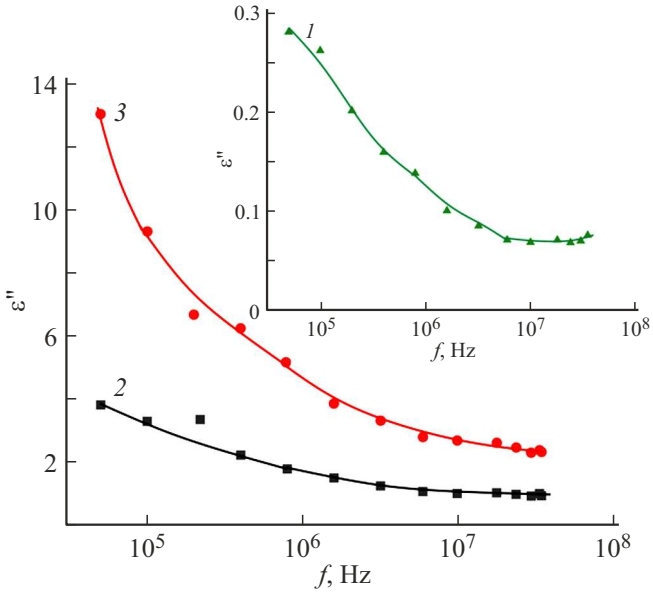

Figure 5. The frequency dependence of the imaginary part of the complex dielectric permittivity ε' of $TlIn_{1-x}Tm_xS_2$ samples of various compositions: $x = 0$ (*1*), 0.001 (*2*) and 0.005 (*3*); $T = 298$ K.

$TlIn_{1-x}Tm_xS_2$ samples. The value of σ_{ac} for samples of $TlIn_{1-x}Tm_xS_2$ was significantly higher than for $TlInS_2$. Two regions were observed on the frequency dependence $\sigma_{ac}(f)$ in $TlInS_2$. Initially, there was a dependence $\sigma_{ac} \sim f^{0.8}$, which then (at $f \geq 10^7$ Hz) changed to the superlinear law $\sigma_{ac} \sim f^{1.2}$.

The law $\sigma_{ac} \sim f^{0.8}$ took place in the frequency range of $5 \cdot 10^4$–$6 \cdot 10^6$ Hz in the sample with $TlIn_{0.999}Tm_{0.001}S_2$ composition while a linear dependence of AC-conductivity on frequency was observed at higher frequencies.

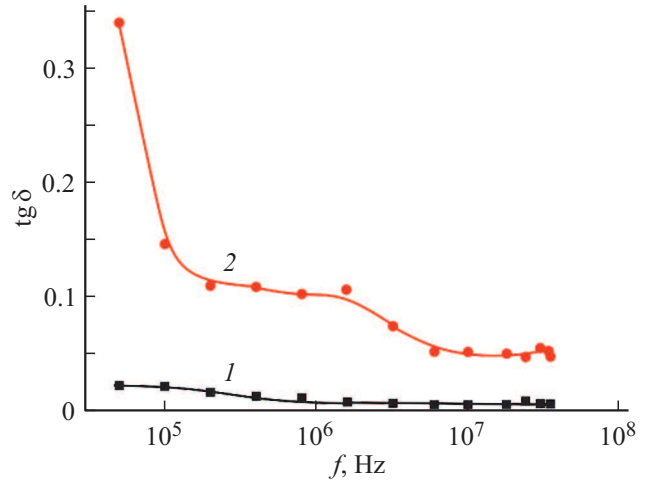

Figure 6. The frequency dependences of the tangent of dielectric loss angle tg δ in $TlInS_2$ (curve *1*) and $TlIn_{0.995}Tm_{0.005}S_2$ (curve *2*); $T = 298$ K.

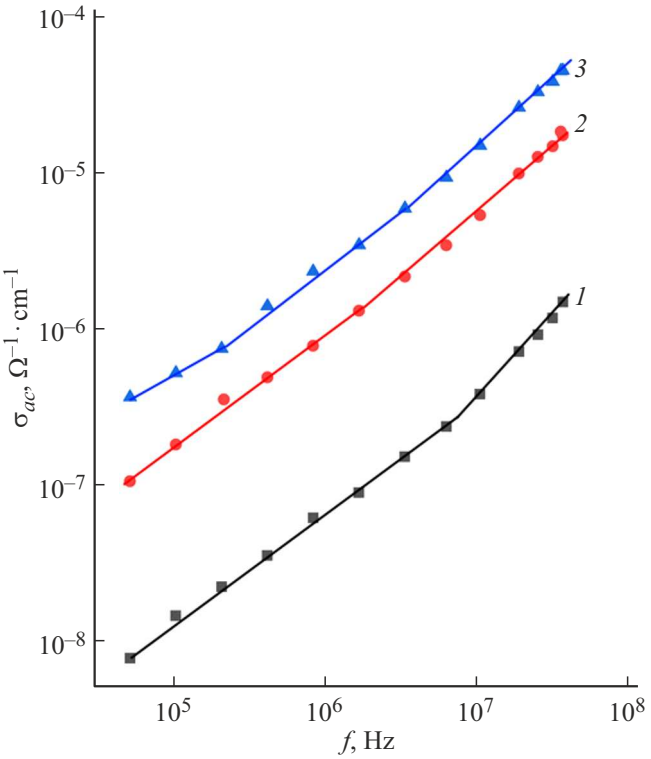

Figure 7. The frequency dependence of the AC conductivity of crystalline samples of $TlIn_{1-x}Tm_xS_2$ of various compositions: $x = 0$ (*1*), 0.001 (*2*) and 0.005 (*3*); $T = 298$ K.

Three sites were observed on the dependence $\sigma_{ac}(f)$ for $TlIn_{0.995}Tm_{0.005}S_2$ composition. Initially, there was a dependence $\sigma_{ac} \cdot f^{0.5}$ up to $2 \cdot 10^5$ Hz which was then replaced by a dependence $\sigma_{ac} \sim f^{0.8}$, and a linear section $\sigma_{ac} \sim f$ was observed with a further increase of the frequency from $6 \cdot 10^6$ Hz to 35 MHz.

Table 2. The parameters of localized states in the crystals of $TlIn_{1-x}Tm_xS_2$ samples calculated using the data of high-frequency dielectric measurements

x	N_F, $eV^{-1} \cdot cm^{-3}$	R, Å	τ, s	ΔE, eV
0	$5.2 \cdot 10^{18}$	86	$2 \cdot 10^{-7}$	0.14
0.001	$1.9 \cdot 10^{19}$	90	$3.3 \cdot 10^{-7}$	0.03
0.005	$3.1 \cdot 10^{19}$	90	$3.3 \cdot 10^{-7}$	0.02

The obtained law $\sigma_{ac} \sim f^{0.8}$ for $TlIn_{1-x}Tm_xS_2$ means a hopping mechanism of charge transfer on states localized in the Fermi level vicinity [19,20]. The density of states at the Fermi level was calculated within the framework of the Mott model using the following formula using the experimentally found values $\sigma_{ac}(f)$ of $TlIn_{1-x}Tm_xS_2$ samples

$$\sigma_{ac}(f) = \frac{\pi^3}{96} e^2 k_B T N_F^2 a_L^5 f \left[\ln\left(\frac{\nu_p h}{f}\right)\right]^4, \qquad (1)$$

where e — the electron charge, k_B — the Boltzmann constant, T — the temperature, N_F — the density of states near the Fermi level, $a_L = 1/\alpha$ — the localization radius; α — the constant of the descending wave function of the localized charge carrier $\psi \sim e^{-\alpha r}$; ν_{ph} — the phonon frequency.

The value $a_L = 14$ Å was taken for the localization radius like in the crystal of $TlInS_2$ [11,19] for calculating the values N_F of samples based on $TlInS_2$ and the value of ν_{ph} is set to 10^{12} Hz [11].

The values N_F calculated for these parameters a_L and ν_{ph} for samples of $TlIn_{1-x}Tm_xS_2$ ($x = 0$, 0.001 and 0.005) are listed in Table 2. Table 2 shows that an increase of the concentration of thulium in $TlIn_{1-x}Tm_xS_2$ results in the increase of the density of states N_F at the Fermi level.

According to the theory of alternating current hopping conductivity of charge carriers in disordered materials the charge carrier average hopping distance R is determined using the following formula [19,20]:

$$R = \frac{1}{2\alpha} \ln\left(\frac{\nu_{ph}}{f}\right). \qquad (2)$$

The value f in the formula (2) corresponds to the average frequency at which $\sigma_{ac} \sim f^{0.8}$ or Mott's law is observed. The values of R calculated using the formula (2) for crystals of $TlIn_{1-x}Tm_xS_2$ are also listed in Table 2. These values R exceed the average distance between the localization centers of charge carriers in $TlIn_{1-x}Tm_xS_2$ crystals in about six times. The value of R made it possible to use the formula

$$\tau^{-1} = \nu_{ph} \cdot \exp(-2\alpha R) \qquad (3)$$

for determining the charge carrier average hopping time in $TlIn_{1-x}Tm_xS_2$ crystals, the values of which are listed in the fourth column of the table.

The following formula [19,20]

$$\Delta E = \frac{3}{2\pi R^3 \cdot N_F} \quad (4)$$

was used for estimation of the energy spread of states localized near the Fermi level in $TlIn_{1-x}Tm_xS_2$ samples (the last column of the table). Table 2 shows that an increase of the concentration of thulium in $TlIn_{1-x}Tm_xS_2$ results in the narrowing of the energy band ΔE, an increase of the density of states N_F at the Fermi level, the average hopping distance and time. Thus, it was found that the introduction of thulium into the crystal lattice of the monoclinic crystal system of $TlInS_2$ modifies the frequency dependences of its dielectric coefficients and the parameters of states localized in the band gap.

4. Conclusion

Optimized structures of supercells based on $TlInS_2$ crystals, obtained from calculations using the DFT method in the LDA, that have monoclinic crystal system (space group $C/2c$, $Z = 16$, № 15) with the corresponding parameters of the lattice cell, are consistent with X-ray phase analysis data of the samples. Doping of $TlIn_{1-x}Tm_xS_2$ samples (for compositions with $x = 0$, 0.001 and 0.005) does result in the formation of any new lines on X-ray phase analysis patterns due to thulium impurity centers. The parameters of the lattice cell of thulium-doped samples of $TlIn_{1-x}Tm_xS_2$ coincide with the parameters of the original $TlInS_2$. All compositions of single crystals of $TlIn_{1-x}Tm_xS_2$ ($x = 0$, 0.001 and 0.005) grown using directional solidification method are formed in monoclinic crystal system (space group C/2c). The lattice constants of $TlInS_2$ crystals found using X-ray phase analysis method have the following values: $a = 10.9017$, $b = 10.9412$, $c = 15.1809$ Å, $\beta = 100.21^{\cdot}$. Thulium introduced into the cation sublattice of the system of $TlIn_{1-x}Tm_xS_2$ ($x = 0.001$ and 0.005) actively affects the dielectric characteristics of the samples.

It was found that thulium doping of the monoclinic structure of $TlInS_2$ results in a significant change of its dielectric properties. An increase of the concentration of Tm x from 0 to 0.005 in case of the cationic substitution in $TlInS_2$ resulted in the noticeable changes of the dielectric permittivity and the tangent of the dielectric loss angle $\mathrm{tg}\,\delta$ in alternating electric fields with a frequency of $f = 5 \cdot 10^4 - 3.5 \cdot 10^7$ Hz at room temperature. In this case, the real and imaginary components of the complex dielectric constant, AC conductivity and loss of reach-through conductivity increase (in more than three times).

The AC conductivity frequency dependence σ_{ac} of $TlIn_{1-x}Tm_xS_2$ samples ($x = 0.001$ and 0.005) at 298 K discovers a hopping charge transfer mechanism. The pattern $\sigma_{ac} \sim f^{0.8}$ that we found in the sample of $TlIn_{0.999}Tm_{0.001}S_2$ composition is characteristic of hopping conductivity. It occurred in the frequency range of $f = 5 \cdot 10^4 - 6 \cdot 10^6$ Hz, and a linear dependence of AC conductivity on frequency was observed at higher frequencies.

The dependence $\sigma_{ac} \sim f^{0.8}$ was observed at frequencies from $2 \cdot 10^5$ to $6 \cdot 10^6$ Hz for $TlIn_{0.995}Tm_{0.005}S_2$ composition and a linear section $\sigma_{ac} \sim f$ occurred in the frequency range from $6 \cdot 10^6$ Hz to 35 MHz. Calculations of the dependence $\sigma_{ac} \sim f^{0.8}$ within the framework of the Mott model show that the introduction of thulium with a concentration of $x = 0.001 - 0.005$ into the crystals of $TlInS_2$ results in the increase of the density of states at the Fermi level ($5.2 \cdot 10^{18} - 3.1 \cdot 10^{19}$ eV^{-1}cm^{-3}), the average distance (86–90 Å) and time ($2 \cdot 10^{-7} - 3.3 \cdot 10^{-7}$ s) of charge carrier hopping from one localized state to another.

Thus, a significant frequency dispersion of the real and imaginary components of the complex dielectric permittivity, the tangent of angle of dielectric losses and AC conductivity at frequencies of $f = 5 \cdot 10^4 - 3.5 \cdot 10^7$ Hz and temperature 298 K was found in the new single-crystal samples of $TlIn_{1-x}Tm_xS_2$ ($x = 0.001$ and 0.005) with monoclinic crystal system that we grew. In other words, the change of the concentration of thulium impurity in $TlInS_2$ crystals makes it possible to modify their dielectric properties.

Conflict of interest

The authors declare that they have no conflict of interest.

References

[1] S.N. Mustafaeva, M.M. Asadov. Phys. Solid State **51**, *11*, 1999 (2004). https://doi.org/10.1134/S1063783419110246.
[2] O.B. Plyushch, A.U. Sheleg. Crystal. Reports **44**, *5*, 813 (1999).
[3] T. Babuka, O.O. Gomonnaic, K.E. Glukhov, L.Yu. Kharkhalis, M. Sznajder, D.R.T. Zahn. Acta Phys. Pol. A **136**, *4*, 640 (2019). https://doi.org/10.12693/APhysPolA.136.
[4] W. Henkel, H.D. Hochheimer, C. Carlone, A. Werner, S. Ves, H.G. von Schnering. Phys. Rev. B **26**, *6*, 3211 (1982). https://doi.org/10.1103/PhysRevB.26.3211.
[5] H. Hahn, B. Wellman. Sci. Nature **54**, *2*, 42 (1967). https://doi.org/10.1007/bf00680166
[6] K.-J. Range, G. Engert, W.A. Muller, A. Weiss. Z. Naturforsch B. **29**, 181 (1974). https://doi.org/10.1515/znb-1974-3-410
[7] T.J. Isaacs, J.D. Feichtner. J. Solid State Chem. **14**, *3*, 260 (1975). https://doi.org/10.1016/0022-4596(75)90030-4
[8] Project 2D Materials Encyclopedia. $TlInS_2$. mp-632539. https://next-gen.materialsproject.org/materials/mp-632539/
[9] S.N. Mustafaeva, M.M. Asadov. Phys. Solid State **51**, *11*, 2269 (2009). https://doi.org/10.1134/S1063783409110122.
[10] A.U. Sheleg, V.V. Shautsova, V.G. Hurtavy, S.N. Mustafaeva. J. Surf. Invest.: X-Ray, Synchrotron and Neutron Techniques. **7**, *6*, 1052 (2013). https://doi.org/10.1134/s1027451013060190.
[11] S.N. Mustafaeva, M.M. Asadov, S.S. Huseynova, N.Z. Gasanov, V.F. Lukichev. Phys. Solid State **64**, *6*, 617 (2022). https://doi.org/ 10.21883/PSS.2022.06.53823.299.

[12] S. Kashida, Y. Kobayashi. J. Phys. Condens. Matter **11**, *4*, 1027 (1999). https://doi.org/10.1088/0953-8984/11/4/010
[13] O.V. Korolik, S.A. Kaabi, K. Gulbinas, A.V. Mazanik, N.A. Drozdov, V. Grivickas. J. Lumin. **187**, 507 (2017). https://doi.org/10.1016/j.jlumin.2017.03.065
[14] V. Grivickas, P. Scajev, V. Bikbajevas, O.V. Korolik, A.V. Mazanik. Phys. Chem. Chem. Phys. **21**, 2102 (2019). https://doi.org/ 10.1039/c8cp06209a
[15] M. Isik, N.M. Gasanly, F. Korkmaz. Phys. B: Condens. Matter **421**, 50 (2013). https://doi.org/10.1016/j.physb.2013.03.046
[16] A.F. Qasrawi, N.M. Gasanly. J. Mater. Sci. **41**, 3569 (2006). https://doi.org/10.1007/s10853-005-5618-0.
[17] K.R. Allakhverdiev, N.D. Akhmed-zade, T.G. Mamedov, T.S. Mamedov, Mir-Gasan Yu. Seidov. Low Temp. Phys. **26**, *1*, 56 (2000). https://doi.org/10.1063/1.593863
[18] M.M. El-Nahass, M.M. Sallam, A.H.S. Abd Al-Wahab. Curr. Appl. Phys. **9**, *2*, 311 (2009). https://doi.org/10.1016/j.cap.2008.02.011
[19] S.N. Mustafaeva, M.M. Asadov, S.S. Huseynova, N.Z. Hasanov, V.F. Lukichev. Phys. Solid State **64**, *6*, 617 (2022). https://doi.org/10.21883/PSS.2022.06.53823.299.
[20] N.F. Mott, E.A. Davis. Electronic Processes in Non-Crystalline Materials. OUP, Oxford, (2012). 590 p. ISBN: 9780199645336

Translated by A.Akhtyamov